

Evaluation of Regular Planar Meshes for Modular Active Cell Robots (MACROs)

Ahsan I. Nawroj, *Student Member, IEEE*, and Aaron M. Dollar, *Senior Member, IEEE*

Abstract— In this paper we investigate a series of candidate regular planar mesh geometries in terms of their suitability for utilization as mesh primitives for constructing compliant robotic structures. In prior work, we established a framework of compliant, articulate robotic meshes, termed Modular Active Cell Robots (MACROs), created from contractile Shape Memory Alloy linear-actuators (Active Cells). In this paper, we examine how to utilize these MACROs and other mesh-like robots in large regular or semi-regular topologies. We evaluate axial strains and stiffness characteristics for a range of MACRO meshes created using different mesh-primitives, which are drawn from known regular space-filling lattice geometries. We then describe the implications of these results on the design of MACRO structures, including the tradeoffs between different primitives for various structural performance properties.

Index Terms—Cellular and Modular Robots, Networked Robots, Simulation and Animation

I. INTRODUCTION

Discrete material robots lie at the exciting intersection of disparate disciplines, aiming at the construction of large-scale robotic mechanisms from groups of discrete, simple, and small robot units. These systems aim towards creating high degree-of-freedom articulable structures from homogeneous components, especially for resource-starved environments, including adjustable cranes for space applications, deconstructible architecture in harsh climates, and other applications (e.g. [1], [2]).

A subclass of discrete material robots are mesh-like robots, where homogeneous components interconnect to create meshes, each leveraging the actions and motions of neighboring robotic components. In prior work, we proposed a class of such systems called Modular Active Cell robots (MACROs) [3], consisting of compliant electro-mechanically deformable meshes. The components of the meshes are simple contractile Shape-Memory Alloy linear-actuators called Active Cells, and passive nodes [4]. We demonstrated the feasibility of using MACROs to create simple robotic mechanisms, and proposed a robust modeling, simulation and control strategy for actuating large instances of MACRO meshes [5].

In this paper, we investigate the use of MACRO meshes to design robotic mechanisms, focusing specifically on a useful design parameter applicable to all periodic meshes: the mesh primitive (Fig. 1(a)-(c)). A considerable literature exists on the

This work was supported in part by the National Science Foundation grant IIS-1317976 and the Air Force Office of Scientific Research grant FA9550-11-1-0093. A.I. Nawroj and A. M. Dollar are at the Department of Mechanical Engineering and Materials Science, Yale University, New Haven, CT, USA. E-mail: {ahsan.nawroj; aaron.dollar}@yale.edu.

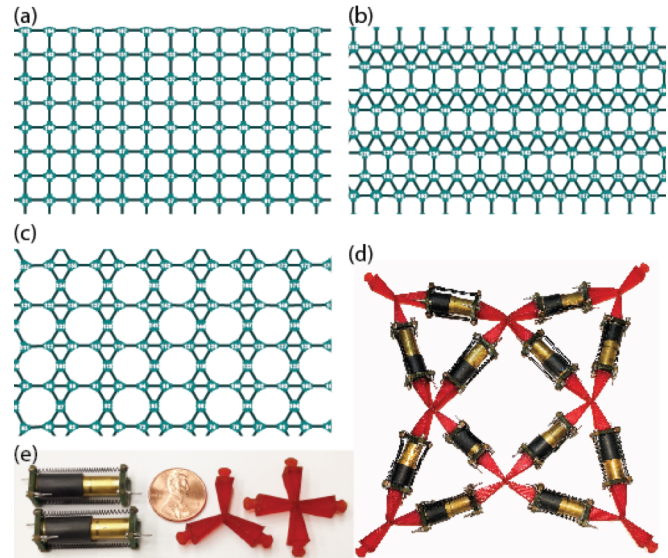


Fig. 1. A series of MACRO meshes using different mesh primitives in periodic pattern (a)-(c). In the MACRO framework using hardware components (d), each of the mesh primitives generate meshes with a set of design tradeoffs in strains from internal actuation and compliance properties in response to externally applied loads. Individual MACRO components (e), including custom SMA-based linear actuators (Active Cells) and molded polyurethane nodes.

effect of meshing and mesh refinement for optimizing material properties and engineering design. We take inspiration from these approaches and apply them to our modular robotic system, which differs from existing work by focusing on meshes that are physically realized using Active Cells, and where both internal actuation as well as external forces contribute to the resulting behavior of a given mesh structure.

We study several mesh primitives by simulating the deformation performance of large MACRO meshes created from each primitive, measuring bulk parameters such as linear strain and axial compressive stiffness. We demonstrate the effect of the choice of mesh primitives in constructing MACRO meshes through a series of simulations, establishing the design tradeoffs incurred for each primitive type.

The rest of the paper is structured as follows: first, we situate our system within the literature of mesh-like and discrete material robots, and geometric studies for a source of mesh primitives (Section II). Next, we describe the MACRO system, including the components of the meshes, and brief overview of prior modeling and control research of such systems (Section III). Then we discuss mesh primitives in some detail, including the selection of primitives both applicable to MACRO meshes and of interest from a geometric perspective (Section IV). In Section V, we describe simulations of MACROs from the selected mesh primitives,

including the results of material property measurements. Next, we discuss the design implications of our testing (Section VI). Finally, we conclude with a summary of findings and future directions of research.

II. RELATED WORK

Mesh-like systems are common in nature and in engineered systems, with physical or virtual links and nodes depending on the application [6]. Several engineered systems also use conceptual links and nodes to formalize the process of design and control, such as formation control of mobile robots [7], coverage control [8], etc. Decentralized solutions tend to produce lower computational cost as the scale of problems increases, using a known communication framework while allowing mesh nodes and edges to move [9]. For some applications, the physical shape of the mesh is an important consideration, such as in tensegrity structures and spatial mechanisms [10].

The study of meshes in isolation from physical systems is also a considerable field, especially from a geometric perspective. This is patently found in truss design [11], topology optimization [12], shape optimization [13], finite element analysis [14], and others.

Increasingly, modular and cell-based robots are using network formulations similar to our own methods. Micro-architected “smart” materials and discrete materials extend this formulation to approximate and enhance naturally occurring as well as processed materials [15], [16].

It is well recognized in all these fields that the shape and topology of physical meshes contribute significantly to their behavior, including stiffnesses and deformations. Our own work attempts to extend this knowledge to the case of internally actuated meshes, where the stiffness and deformation properties can be dynamically adjusted by applying power to the boundary of the meshes. We believe that electronic control methods for mesh shape control as well as the topology and geometry used in the design of the mesh can work together to affect physical properties that would not be easily possible with either approach alone.

III. THE MACRO SYSTEM

Modular Active Cell Robots (MACROs) are discrete material robots consisting of deformable meshes created from Active Cells and passive compliant nodes. MACROs are structural robots, designed to provide shape-changing ability to a robotic material. The shape-change in a MACRO mesh is caused by internal actuation of the active elements in the mesh, as well as an ability to respond to environmental forces. The edges of the mesh consist of scalable custom linear-actuators made from SMA coils and passive springs: Active Cells [4]. The nodes of the MACRO mesh consist of passive, compliant, elastomeric torsional joints, which can attach to two or more Active Cells depending on the number of arms molded into the node. The individual components of the MACRO system are shown in Fig. 1(e). It should be noted that a MACRO consists of electrical components to power and actuate the robotic mesh in addition to the mesh of cells and nodes itself; however, since in this paper we focus on the mechanical performance of various mesh connectivity patterns, we refer to MACROs and meshes interchangeably.

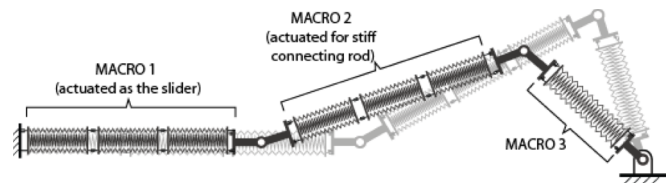


Fig. 2. Diagram of a simple multi-module MACRO. The slider-rocker’s initial rest position is shown in gray. The actuated position is shown in black. Each individual MACRO can be actuated separately, and can be constructed from different mesh primitives.

MACROs are activated by voltages set at two or more nodes of the mesh. Each passive compliant node also provides access to external power, and all nodes are electrically conductive to neighboring cells: two cells mechanically connected at a passive node are electrically connected as well. Clearly, as the size of the MACRO grows, the number of nodes increases depending on the connectivity of the mesh. It would be impractical to define the robotic structure with necessary wire access to every internal node of the mesh. Thus, in all our work, we use the boundary nodes only in providing currents to the system and controlling the shape of the MACRO.

The modularity of MACROs is evident in terms of the electrical and mechanical connectivity of multiple meshes. Two MACRO meshes, each with a mechanical connectivity configuration, electrical connections and power inputs, can connect to each other along the boundary of each mesh. This is useful for separating mechanical behavior of a complex mechanism into discretized modules that perform a specific single task. For example, a simple MACRO-based slider-rocker mechanism can consist of three MACRO modules: a rocker, a connecting rod, and a slider (shown diagrammatically in Fig. 2). Each of these meshes connect in series along specific boundary nodes of the mesh, and are electrically isolated from each other. During operation, the connecting rod and rocker can be actuated to create a pair of rigid links, while the slider can be actuated periodically to give oscillating motion.

We have provided hardware demonstrations of the MACRO concept by fabricating Active Cells and passive nodes and using boundary-node activation to cause observable deformations. It is important to note that the fabricated cells and nodes do not represent the only instantiation of the MACRO framework for creating mesh robots. In fact, the choice of SMA-based cells is itself a design choice on our part. The generalized MACRO framework applies equally well to any mesh robot having actuated edges and passive compliant nodes.

While it is possible to study the behavior of MACRO meshes in hardware, from a practical standpoint, this becomes unwieldy as the scale of the structure grows. Thus, we have characterized the SMA-based Active Cell in some detail and modeled the behavior of resultant MACRO meshes given boundary-node voltages and connectivity configurations. This model was validated against hardware trials [3], and the modeling and simulation of electrical and mechanical response of the system was established to be an adequate substitute for the hardware instances in terms of the low-bandwidth bulk-properties of any given MACRO.

IV. MESH PRIMITIVES

The MACRO framework applies the following constraints on a mesh configuration:

- Polygons enclosed by cells in the mesh are regular at rest. The edges of the framework are identical. Thus, each shape formed by the cells are polygonal and regular while at rest. During actuation, the regularity of the polygons will, in general, change, but if all cells are at identical states, the resulting polygons will remain regular.
- Polygons enclosed by cells tile edge-to-edge: Since connections between adjacent polygons enclosed by cells can only happen at the passive nodes, the edge-to-edge constraint is implied.
- Vertex transitivity: All vertices of the mesh of a given MACRO are connected to identical number of cells. While not strictly required by the framework, this is a useful generalization for rapid fabrication since only one type of molded node need be used for a given MACRO. A complex mesh that requires non-transitive vertices to account for geometric needs can be considered as a MACRO consisting of two or more MACRO modules, each of which has vertex transitivity.

Mesh primitives are defined to be small structures of Active Cells and nodes that is the “unit cell” of a mesh, i.e. the mesh can be described as a periodic tiling of this mesh primitive within a specific boundary profile. In general, the mesh primitive can be described by a few adjacent polygons enclosed by cells in the mesh.

The combination of the constraints above imply that mesh primitives must be connected in uniform tiling patterns. There are three mesh primitives that are uniform regular tilings of the plane and use a single polygon in their structure: the hexagon primitive, the square primitive, and the triangle primitive (Fig. 3). We refer to these as the simple mesh primitives.

There are eight mesh primitives that are uniform semi-regular tilings of the plane, i.e. they use more than one regular polygon in their structure (Fig. 4). We refer to these as the hybrid mesh primitives.

We construct large MACRO meshes using simple and hybrid mesh primitives, simulating their behavior when actuated using a simple voltage setting along the boundary of these meshes. The key issues we attempt to resolve using this research are:

- The significance of differences between the different mesh primitives for design applications
- The impact of mesh primitive choice on shape change capability for a given amount of power input to the MACRO mesh
- The impact of mesh primitive choice on stiffness (or compliance) of the MACRO mesh

The series of simulated trials of each large mesh instance as well as the results of the physical measurements, are described in the following section.

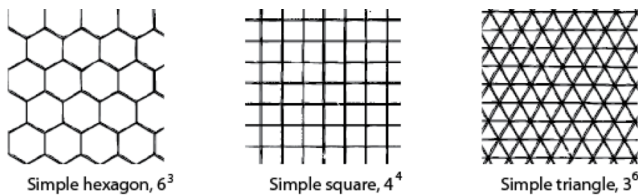


Fig. 3. The 3 uniform-regular tilings of the plane [17]. Each of tilings are used as simple mesh primitives.

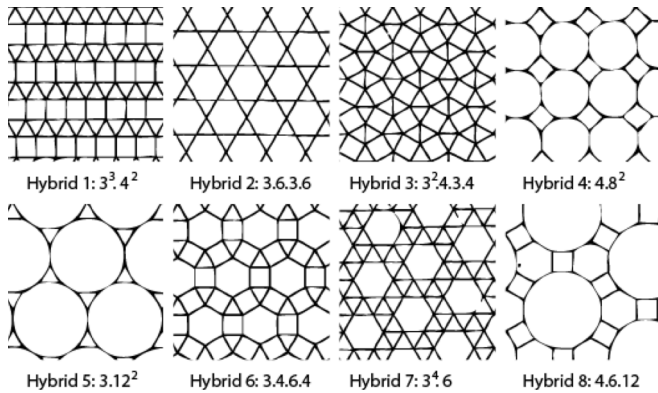


Fig. 4. The 8 uniform-semi-regular tilings of the plane [17]. Two of these tilings are used as “hybrid” mesh primitives (Hybrid 1 and 2).

Since one of the purposes of a MACRO mesh is to provide specific deformations, we identify two avenues of providing deformation control:

- The mechanical connectivity of the mesh components during the construction of the mesh.
- The application of boundary-nodal voltages in any given mesh to actuate specific groups of Active Cells

The latter is explored in concurrent research through the development of a robust, simple and scalable control strategy for setting nodal voltages that minimizes the error between the shape of a MACRO mesh and a given shape it is meant to approximate [5].

In this paper, we study the former approach using the computational MACRO model. We study the effect of a specific design variation in constructing meshes: the connectivity configuration. It is possible to construct arbitrary connections of Active Cells and nodes as a MACRO mesh, and then use electronic control to provide motion to match shapes as desired. However, there are two complications with this naïve approach. First, access to only the boundary-nodes to control the shape (positions and relative distances between nodes) of the entire mesh can be an under-defined or over-defined problem depending on the number of nodes and edges in the mesh, and it is possible that the desired shape requires actuation in an uncontrollable and unobservable direction. Second, some shape changes might be possible but require high currents to flow across nodes to undergo extreme edge contractions in one connectivity configuration, while requiring virtually no effort to maintain shape for another connectivity configuration; for example, it is far easier to approximate an irregular triangle using a triangular mesh configuration than using a rectangular mesh configuration.

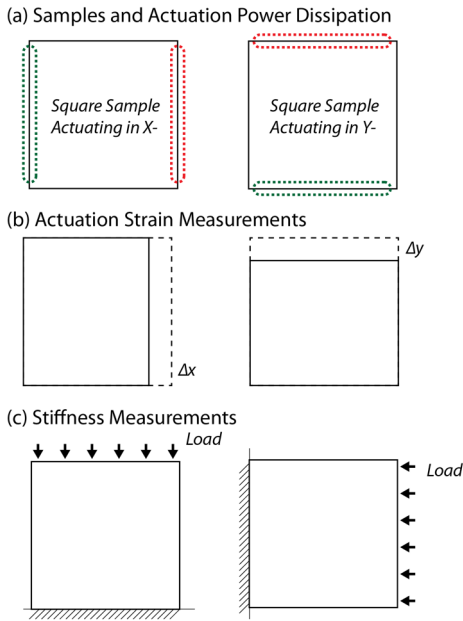


Fig. 5. Test conditions used in simulated experiments. (a) Samples sizes and actuation conditions. (b) Strain measurements for the samples. (c) Stiffness measurements through the application of simulated loads on the boundary of the samples.

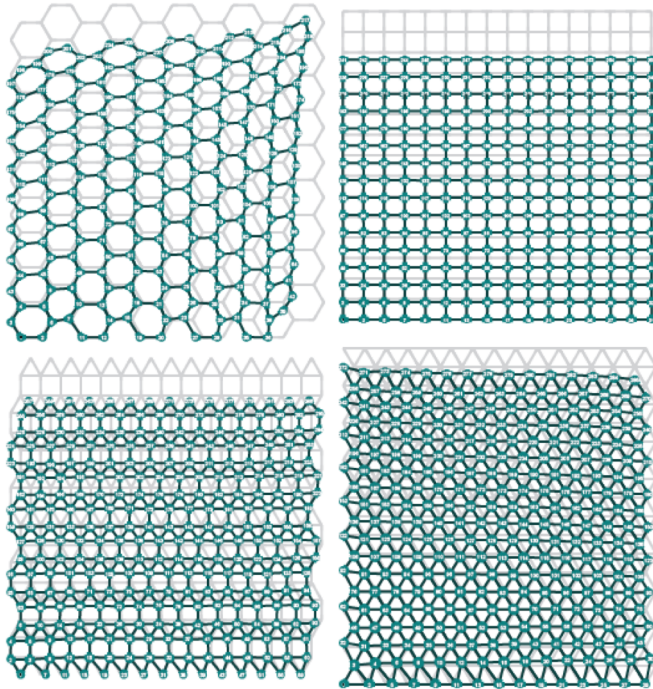


Fig. 6. The large meshes constructed for each of the five tested mesh primitives (top-left: hexagon, top-right: square, bottom-left: hybrid 1, bottom-right: triangle). The deformations are in green, while the rest state is shown in gray. Each of the selected deformations are shown for actuation along the y- axis (current applied between the top and bottom nodes).

V. TEST OF MESH PRIMITIVES AND RESULTS

In each of the simulated trials, we select one of the mesh primitives, and tile a square on the plane that is 15x15 cells in length (Fig. 5). When the primitive has irregular boundaries, the number of primitive instances used in the tiling is computed for each primitive to minimally cover the test square

TABLE I PARAMETERS OF SIMULATION TRIALS

Name	# primitives in x-	# primitives in y-	# nodes in mesh	# cells in mesh
Hexagon	$n = \frac{2(d-0.5)}{3}$	$n = \frac{d}{\sqrt{3}}$	218	307
Square	$n = d$	$n = d$	256	480
Triangle	$n = 2(d-1)$	$n = \frac{2d}{\sqrt{3}}$	285	788
Hybrid 1 (3 ³ .4 ²)	$n = d$	$n = \frac{d-\sqrt{3}/2}{1+\sqrt{3}/2}$	286	645
Hybrid 2 (3.6.3.6)	$n = \frac{d-1}{2}$	$n = \frac{d}{\sqrt{3}}$	222	410

Note: In the equations above d refers to a distance in cell lengths to be tiled by each mesh primitive, and n is the number of primitive instances required to tile this distance.

sample. For each mesh primitive, the number cells and nodes are listed on TABLE I. The table also includes a simple pair of equations for generating the number of primitive instances required to generate a tiling pattern to fit a square sample size.

For each sample, two experiments are performed in simulation, actuating the sample along the x- and y- axis. For actuation along the x-axis, nodal voltages are set up on the nodes on the left and right borders of the sample such that a constant current of 1A flows from left to right. The computation of these voltages is described in [3]. Similarly, for actuation along the y-axis, nodes along the top- and bottom-edge of the sample are set to voltages to drive 1A between these two surfaces.

For each trial (sample and actuation direction), the overall actuation stroke is calculated from the rest configuration. Additionally, for each trial, the stiffness of the mesh is computed by exerting a 1N distributed load along the right/top edge (while the left/bottom edge respectively is held with a rigid constraint). Thus, a bulk stiffness measure is taken along the x- and y- axis for each trial. The measurements are taken at the start of actuation as well as at the end of actuation. The samples and the measurements for the simulated experiments are shown diagrammatically in Fig. 5, while the results of four trials are shown in Fig. 6.

The MACRO modeling and simulation includes an element of noise to be physically realistic and account for measurement errors. We therefore run 10 trials for each mesh primitive and actuation direction, resulting in 20 trials per mesh primitive. SMA is a low-bandwidth actuator, and the trial length is set at 10s for all meshes, to allow the meshes to complete deforming under the constant input power.

The bulk strain along the x- and y- axis of the mesh for the simulated trials are shown on Fig. 7. The results are segmented by the mesh primitive types tested.

The bulk stiffness along the x- and y- axis of the mesh for the simulated trials at the start of the trial are shown on Fig. 8. The bulk stiffness measurements for the mesh at the end of the actuation are shown on Fig. 9. We discuss the results of the trials – especially in terms of design implications of mesh primitive selection – in the following section.

VI. DESIGN IMPLICATIONS OF PRIMITIVE SELECTION

From Fig. 7, mesh primitive selection is shown to produce significant variations in bulk strain. The highest strain in both x- and y- directions of actuation is observed for the square

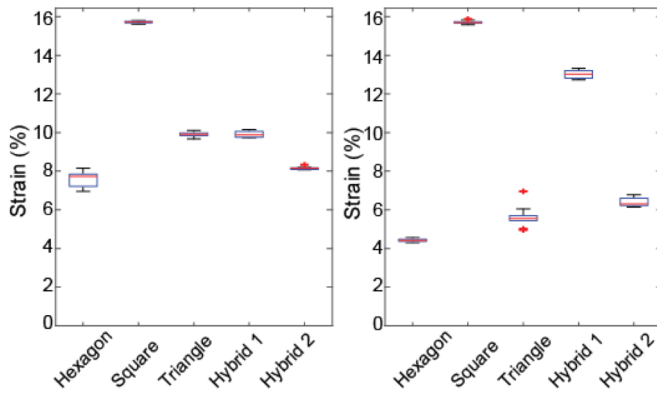


Fig. 7. Bulk-strain along x- and y-axis, shown segmented by type of mesh primitives.

primitive, which supports the intuitive hypothesis that alignment of cells along the direction of actuation increases strain along that direction. Additionally, the square primitive produces comparable strains along each axis, which matches the symmetric structure of the primitive.

The bulk strains along x- and y- are not equivalent for most of the primitives, however. This is most pronounced for the primitives that contain triangular polygons (simple triangle and the hybrids). Since triangular polygons are not congruent about the two axes of actuation, the bulk strains for the primitives are similarly different. In fact, for a single upright triangle, the strain along the y-axis (along the “height”) is expected to be 62.4% of the strain along the x-axis (along one of the sides). For the simple triangular primitive, the strain along y- is $5.6 \pm 0.6\%$, whereas the strain along x- is $9.9 \pm 0.1\%$, a ratio of $\sim 56.8\%$.

From Fig. 8, we can compare the stiffness of the MACRO meshes at rest. Intuitively, the stiffness of the meshes are likely to be most closely related to the topology of the mesh primitives at this time, since they most strongly resemble the theoretical tiling at $t = 0$.

We observe that the hexagon primitive is the least stiff of the tested primitives, along both axes of measurement. This is accounted for by the sparse structure of this primitive, as well as the high degree of branching. Powering the hexagonal primitive along either axis always causes deformation along the perpendicular axis as well; the deformed structure of two trials of the hexagon primitive are shown on Fig. 10 to illustrate this idea.

The hybrid 1 primitive uses a mixture of squares and triangles, and the resultant meshes have comparable stiffness to the simple square and triangle primitives. The hybrid 1 has strain along y- that is $7.4 \pm 0.4\%$ higher than for simple triangle, and $2.7 \pm 0.1\%$ lower than the simple square.

The hybrid 2 primitive, using hexagons and triangles, has higher stiffness than the simple hexagon primitive due to the triangles acting as bracing structures (stiffness increase of $0.6 \pm 0.3\%$ along x- and $2.0 \pm 0.1\%$ along y- when compared to the simple hexagonal primitive).

As the meshes deform from internal forces, the stiffness of the meshes vary. This is visualized on Fig. 9. Interestingly, every primitive has considerably lower stiffness once the mesh is activated (compared to stiffness at rest state). This is

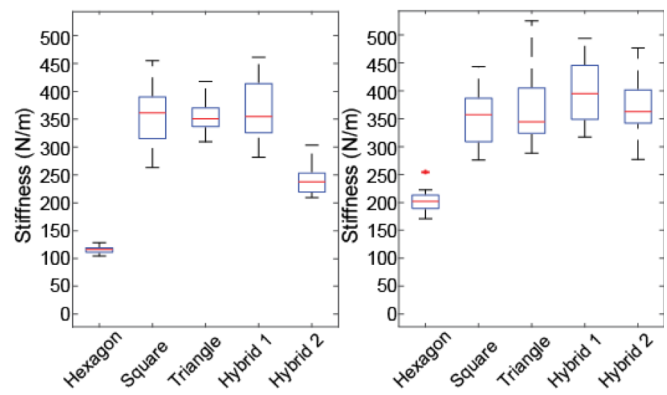


Fig. 8. Compressive stiffness at the start of trial ($t = 1s$), shown segmented by type of mesh primitives. Left plot shows stiffness along x-, right plot shows stiffness along y-.

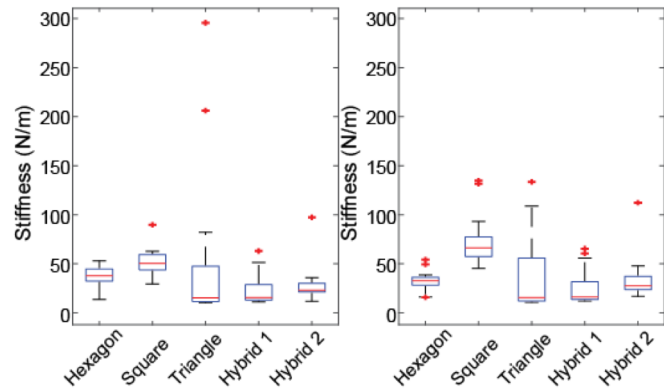


Fig. 9. Compressive stiffness at the end of trial ($t = 10s$), shown segmented by type of mesh primitives. Left plot shows stiffness along x-, right plot shows stiffness along y-.

noteworthy because it is unlike most bulk materials, where the stiffness increases with compression.

This unusual phenomenon is a consequence of the way MACRO meshes deform and respond to forces. When a MACRO is at rest, the cells and nodes are arranged in a regular pattern, and the sparseness and connectivity of the components contribute to a measure of stiffness of the structure. When the structure is powered, the cells increase in stiffness while the passive nodes remain equally stiff. Since the nodes have considerably lower stiffness than cells (to allow for high articulation of the structure), the structure becomes more compliant to external forces as the regular patterns become increasingly more dislocated. This is the inverse of the

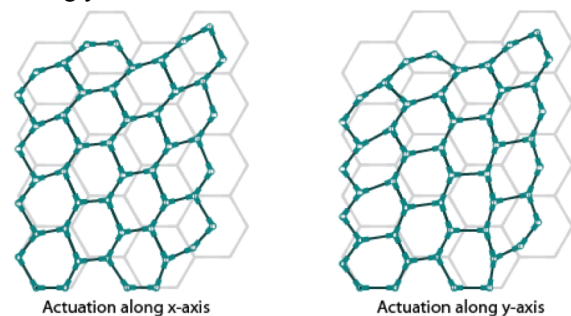


Fig. 10. Start and deformed positions for a small hexagonal mesh actuated along x- and y- axes. The hexagon primitive is branched symmetrically along the x- and y- axes, and thus power application along either dimension collapses the entire structure in a similar fashion.

presence of grain boundaries in latticed physical materials. When grain boundaries are aligned in opposition to external forces (boundary nearly perpendicular to applied force), the material is in compression and stiff. When grain boundaries are aligned to take advantage of shear (boundary in line with force), the layers can slide and the material is more compliant. Similarly, when an actuated MACRO is in compression, the applied force is more likely to deform through nodal torsion rather than cell compression. This effect is so pronounced (actuated cell stiffness much greater than node torsional stiffness), that all primitives demonstrate very low bulk stiffness when actuated.

The combination of these factors contributes to a set of design tradeoffs for each mesh primitive type. High strains are best obtained from regular simple mesh structures, such as the simple square or hybrid 1 primitives. High axial stiffness is best obtained from a square or a triangulation, such as simple triangle primitive, simple square or hybrid 1.

In many applications, high compliance is more important than strain. In such cases, the hexagonal primitive is appropriate. Depending on the tasks a given mechanism needs to perform, multiple MACROs with different mesh primitives may be appropriate to use.

VII. CONCLUSIONS

We have described the use of mesh construction through primitive selection as a method of controlling the bulk material properties of compliant mesh-robots. Tested mesh primitives demonstrate varying strains and compressive stiffnesses along the x- and y- axes for identical test conditions: different choice of primitives have up to 12% difference in axial strain, and up to 355 N/m difference in compressive stiffness.

In future work, we plan to continue testing more semi-regular mesh primitives, as well as study the effect of varying nodal torsion to affect unactuated vs. actuated mesh instances. We also plan to apply the research on mesh primitives to the design and control of mechanisms constructed using MACROs.

REFERENCES

- [1] K. C. Cheung and N. Gershenfeld, "Reversibly Assembled Cellular Composite Materials," *Science (80-)*, vol. 341, no. 6151, pp. 1219–1221, Sep. 2013.
- [2] T. A. Schaedler, A. J. Jacobsen, A. Torrents, A. E. Sorensen, J. Lian, J. R. Greer, L. Valdevit, and W. B. Carter, "Ultralight Metallic Microlattices," *Science (80-)*, vol. 334, no. 6058, pp. 962–965, Nov. 2011.
- [3] A. I. Nawroj, J. P. Swensen, and A. M. Dollar, "Towards Modular Active-Cell Robots (MACROs): SMA Cell Design and Modeling of Compliant , Articulated Meshes," *IEEE Trans. Robot.*, 2017.
- [4] A. I. Nawroj, J. P. Swensen, and A. M. Dollar, "Design of mesoscale active cells for networked, compliant robotic structures," in *2015 IEEE/RSJ International Conference on Intelligent Robots and Systems (IROS)*, 2015, vol. 2015–Decem, pp. 3284–3289.
- [5] A. I. Nawroj and A. M. Dollar, "Shape Control of Compliant , Articulated Meshes : Towards Modular Active-Cell Robots (MACROs)," in *IEEE Robotics and Automation Letters*, 2017.
- [6] V. Kumar, D. Rus, and G. S. Sukhatme, "Networked Robots," in *Springer Handbook of Robotics*, Berlin, Heidelberg: Springer Berlin Heidelberg, 2008, pp. 943–958.
- [7] K. Kanjanawanishkul, "Formation control of mobile robots: survey," *Eng. Ubu. Ac. Th*, pp. 50–64, 2005.
- [8] J. Cortes, S. Martinez, T. Karatas, and F. Bullo, "Coverage control for mobile sensing networks," in *Proceedings 2002 IEEE International*

- Conference on Robotics and Automation (Cat. No.02CH37292)*, 2002, vol. 2, no. May, pp. 1327–1332.
- [9] A. Jadbabaie, J. Lin, and A. S. Morse, "Coordination of groups of mobile autonomous agents using nearest neighbor rules," *IEEE Trans. Automat. Contr.*, vol. 48, no. 6, pp. 988–1001, Jun. 2003.
- [10] C. Paul, F. J. Valero-Cuevas, and H. Lipson, "Design and control of tensegrity robots for locomotion," *IEEE Trans. Robot.*, vol. 22, no. 5, pp. 944–957, 2006.
- [11] C. A. Coello and A. D. Christiansen, "Multiobjective optimization of trusses using genetic algorithms," *Comput. Struct.*, vol. 75, no. 6, pp. 647–660, 2000.
- [12] G. Bianchi, M. Harders, and G. Székely, "Mesh Topology Identification for Mass-Spring Models," *Med. Image Comput. Comput. Interv. MICCAI 2003*, vol. 1, pp. 50–58, 2003.
- [13] J. A. Hetrick and S. Kota, "An Energy Formulation for Parametric Size and Shape Optimization of Compliant Mechanisms," *J. Mech. Des.*, vol. 121, no. 2, p. 229, 1999.
- [14] K. Ho-Le, "Finite element mesh generation methods: a review and classification," *Comput. Des.*, vol. 20, no. 1, pp. 27–38, 1988.
- [15] L. A. Shaw and J. B. Hopkins, "An Actively Controlled Shape-morphing Compliant Microarchitected Material," *J. Mech. Robot.*, vol. 8, no. c, p. 21019, Nov. 2015.
- [16] B. Haghpanah, H. Ebrahimi, D. Mousanezhad, J. Hopkins, and A. Vaziri, "Programmable Elastic Metamaterials," *Adv. Eng. Mater.*, pp. 1–7, 2015.
- [17] B. Grünbaum and G. C. Shephard, "Tilings by Regular Polygons," *Math. Mag.*, vol. 50, no. 5, p. 227, Nov. 1977.